

Diffusion of Spherical Polystyrene Particles through a Tilted Washboard Potential

Undergraduate Researcher
Aaron J. Midkiff, University of Washington

Faculty Mentor
John B. Ketterson
Department of Physics and Astronomy,
Northwestern University

Graduate Student Mentor
Weiqiang Mu
Department of Physics and Astronomy,
Northwestern University

Abstract

This project involved the study of Brownian motion of polystyrene microspheres in the presence of gravity and a one-dimensional sinusoidal optical potential generated by the interference of two laser beams. An exponential relationship was observed between applied laser power and particle residence time of individual interference fringes. Increasing laser power also revealed a wider distribution of residence times and a more narrow distribution of displacements from the $t = 0$ position. These observations were confirmed using finite-difference time-domain (FDTD) computer simulations.

Introduction

A powerful laser beam directed on macroscopic objects, though capable of delivering blistering intensity and causing damage, is still not capable of exerting much force on the object. However, when one deals with objects on the scale of microns and smaller, the optical forces arising from a focused laser beam are comparable in magnitude to gravity and accordingly can be observed and measured directly; in particular, they can be used to suspend and manipulate the motion of objects.

The mechanism behind this optical force is the conservation of momentum. When laser light is incident upon a surface (such as that of a polystyrene particle), it is deflected (scattered) and changes direction. This change of direction is equivalent to a change in momentum of the light that in turn results in an optical force upon the particle. The motion imparted to the particle follows from Newton's law:

$$\frac{dp}{dt} = \frac{d}{dt}(mv) = m * \frac{dv}{dt} = m * a = F_{\text{optical}}.$$

There are two components to the optical force, F_{optical} . The first component is the scattering force¹:

$$F_{\text{scat}} = \frac{n_p P_{\text{scat}}}{c},$$

where n_p is the index of refraction of the particle being observed, and P_{scat} is the power scattered. The trend of the scattering force is to push an object in the path of the laser along the direction of propagation of the beam. However, even though this force was present in our experiments, it did not play a significant role in the structure of the potential (because the slide plates housing the sample stands in the path of the laser, as shown in Figure 5, the slides act as a brick wall stifling the motion of the particle along the direction of the laser — there is only motion in the plane of the sample slide), so it will be set aside for the time being.

The portion of the optical force playing a primary role in the shape of the washboard potential is the gradient force. Quantitatively this force is given in the following form:¹

$$F_{\text{grad}} = -\frac{n_p}{2} \alpha \nabla E^2,$$

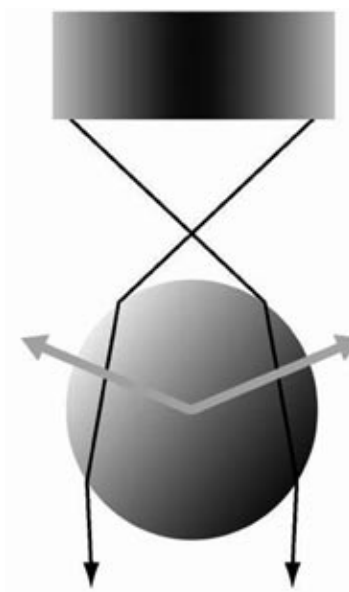
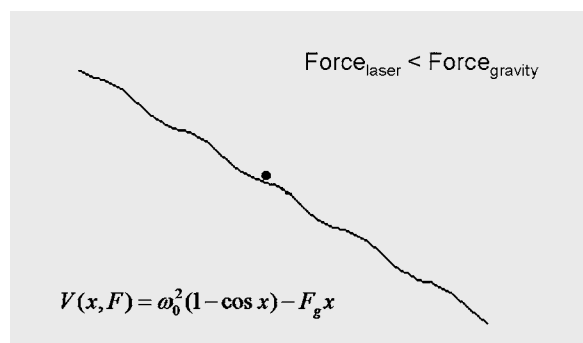
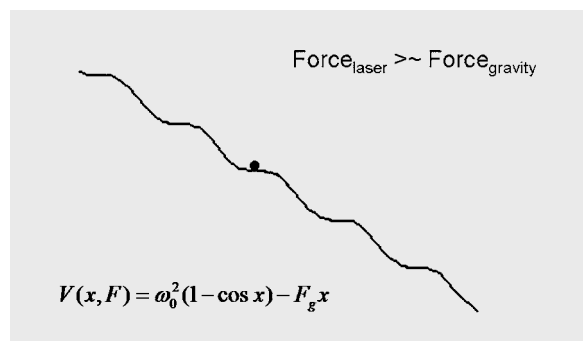
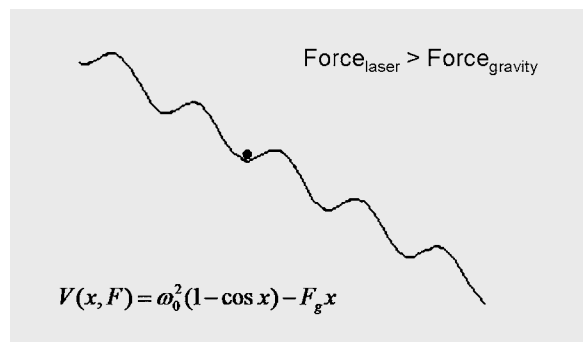


Figure 1: Gradient force due to incident light beams upon particle. The shading across the lens indicates an intensity gradient across the beam, with maxima located along the beam axis. The black lines are incident and scattered light passing through the particle. The gradient force brought about here has equal and opposite radial components (gray lines).⁷

Diffusion of Spherical Polystyrene Particles through a Tilted Washboard Potential (*continued*)



Figures 2–4: Washboard potential illustration. Shown are three instances of differing washboard potential amplitude: i) Force due to the standing wave of the laser is dominant compared with the force of gravity. A particle is completely confined to the potential well and unable to escape. ii) With a weakened standing wave amplitude, the magnitude of gravity is comparable to that of standing wave. The particle is confined at times but is able to escape at times. iii) The standing wave amplitude is miniscule compared with gravity, as the particle freely diffuses without ever being confined to a potential well.

where α is the polarizability of the particle of interest. This force arises from a gradient in the intensity over the cross-section of the beam. The direction of the gradient force is dependent upon the relative indices of refraction of the particle and the surrounding medium, as shown in Figure 1. When the index of refraction of the particle is greater than that of the medium within which it is suspended, the gradient force points toward the region where the beam intensity is maximal, which represents the potential minimum and is located along the beam axis. The exact opposite is true when the index of the medium is larger than that of the particle; here, the particle would be repelled outward from the center of the beam. This can be referred to as a repulsive radiative force.²

Another physical phenomenon exploited in these experiments is a set of interference fringes generated by two intersecting laser beams. In the case of a Gaussian laser light beam, one has interference fringes with the peak intensity in the center of the pattern and the gradient and scattering forces that accompany it. In the present experiments the scattering force is opposed by the presence of a glass sample slide plate, as noted above. When the laser intensity is sufficiently low, the gradient force can be comparable in magnitude to the force of gravity acting upon the particle. It is in this regime that we will characterize the movement of a particle subject to a combination of these two forces (picturesquely described as “fall in a washboard potential,” seen in Figures 2–4).

Background

The past decade has seen an explosion in the use of laser light to trap particles that are microns in diameter and smaller. Such work has paved the way for biological applications; perhaps the most famous of these is the manipulation of DNA molecules. These so-called optical tweezers allow significantly improved control in carrying out such processes, while inflicting minimal, if any, damage on the object.³

This field of optical tweezing was initiated by Arthur Ashkin, who laid its foundations in a 1970 publication while he was working at Bell Laboratories.⁴ His paper was the first to discuss the trapping of particles with radiation pressure generated by visible laser light. By focusing a 1 watt cw argon laser operating at a wavelength of 514.5 nm, Ashkin successfully trapped transparent

latex spheres with several different radii. The spheres were suspended in water. In a 1986 publication, Ashkin made the first observation of trapping of dielectric particles by using the gradient force of an argon laser, the same method used in our experiments.

More recently, and specific to this work, is the work of Constantini and Marchesoni on the dynamics of a Brownian particle in a tilted washboard potential. The equation describing the forces experienced by the particle is^{5,6}

$$\ddot{x} = -\gamma\dot{x} - \omega_0^2 \sin x + g + \zeta(t),$$

where the terms on the right hand side correspond to a viscous drag (characterized by a constant γ), a spatially periodic optical acceleration, the acceleration due to gravity, and a random (Gaussian) acceleration (also called noise). The noise is particle motion due to collision

with particles of the medium within which it is suspended; this is referred to as Brownian motion. A particle whose motion is dominated by this noise (occurring as the particle radius shrinks beyond a certain limit) is referred to as a Brownian particle. A method to describe the average position is to model the Brownian particle's position as that for the density of a concentrated drop of one liquid diffusing into a second (background) liquid. In the absence of gravity and the washboard potential, the resulting analytic expression is a solution to the well-known diffusion equation with a delta function source. With the two added forces, the one-dimensional diffusion equation takes on the form

$$\frac{\partial \rho}{\partial t} = D \frac{\partial^2 \rho}{\partial x^2} - f \frac{\partial \rho}{\partial x} - \rho \frac{\partial f}{\partial x},$$

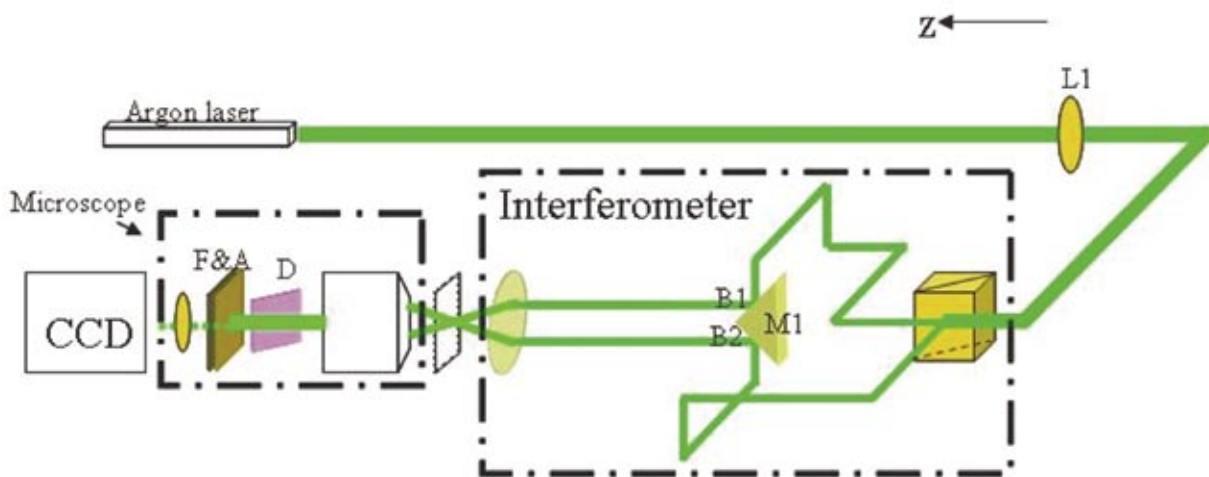


Figure 5: Optical setup. The argon laser is reflected and split into portions offset in pathlength that interfere with one another and provide the horizontal interference fringes shown in Figure 8. L stands for lens, B for beam, M for mirror, D for diaphragm, and F and A are filter and attenuator. The placement of mirrors is implied where the beam changes direction.

Diffusion of Spherical Polystyrene Particles through a Tilted Washboard Potential (*continued*)

where ρ is the probability density of the particle (with respect to position and time), D is the diffusion constant, and f is proportional to the difference between the force due to gravity and force exerted by the interference fringes ($f \propto mg - \omega_0^2 \sin x$). The solution is found by numerical integration (in this case using finite difference time domain [FDTD] simulations) from which the ratio of backward to forward jumps can be derived.

Approach

We placed a very simple “spin” on the experiments described in Ashkin’s 1986 publication. Lowering the beam intensity, the gradient force exerted upon the particle by the laser was comparable in magnitude to the force of gravity — so comparable in fact that gravity gradually overcame the gradient force, and we were able to observe the diffusion

of the particle through the horizontal interference fringe pattern. This unique combination of forces is what we refer to as a “tilted washboard potential.” It gets this name from the combination of the standing wave pattern created by the laser and the vertical force of gravity, which combine to give a series of potential maxima and minima tilted at an angle within which we observe the particle shake back and forth under random thermal impacts during its fall through the series of interference fringes. The washboard potential is described by the following analytic expression:

$$V(x, F) = \omega_0^2(1 - \cos x) - F_g x,$$

where ω_0 is proportional to the intensity of the laser, and F_g is the force due to gravity.

The experiments in this paper were performed using spherical polystyrene particles three microns in diameter suspended in deionized water, and an argon laser operating from 7 to 31 milliwatts at 514.5 nm in the TE₀₀ mode (optimized for uniformity of the washboard potential); all components were mounted atop an air-cushioned optical table. Using the experimental setup of lenses, mirrors, beam splitters, etc., shown in Figure 5, the argon beam was split into four nominally equal intensity beams. Two of these were used to create a set of vertical interference fringes, while the other two created a horizontal set (for the present experiments, where we sought only to observe particle diffusion through one-dimensional, horizontal fringes, the two beams creating the vertical set of interference fringes were blocked). All experiments were viewed and/or recorded by a CCD directly behind the sample. Photographs of the particle diffusion are seen in Figure 10.

All of the polystyrene particles used here carry an inherent negative charge, resulting in a repulsive Coulomb force between neighboring particles that prevents clustering. This allowed for the simultaneous observation of the descent of several particles simultaneously, with the results minimally skewed by occasional particle encounters. The slide plates also bear an inherent negative charge. This, along with the near sterile state of the slides prior to use, minimized adhesion of the polystyrene particles to the sample slide plate so long as the scattering force magnitude was not large enough to significantly displace particles and a freshly refrigerated sample was used.

Due to the Gaussian intensity distribution spread over the cross-section of the laser, only a small region (roughly

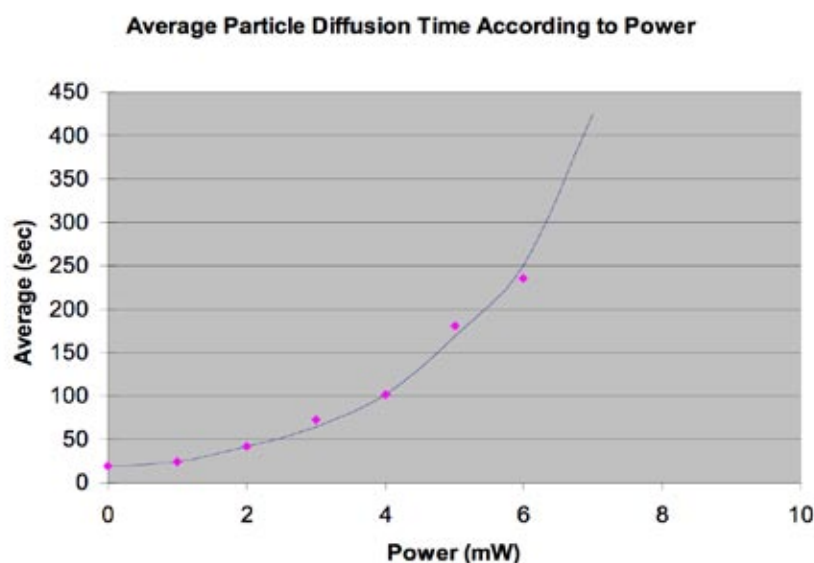


Figure 6: Average diffusion time for increasing laser intensity. The small diamonds are data points with average error bars. The function in the background of the plot is an exponential model.

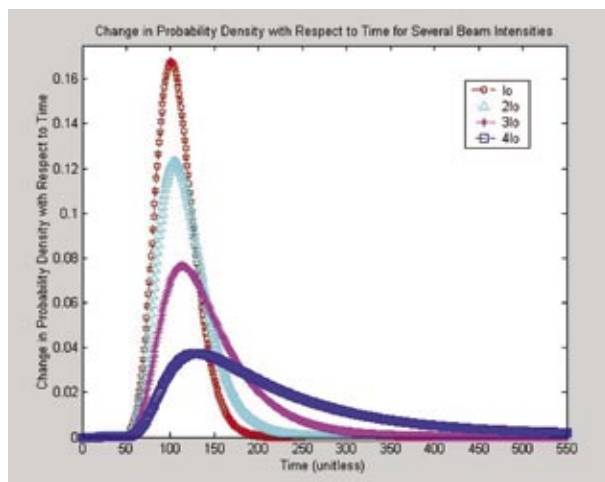


Figure 7: Change in probability density against time for increasing laser intensity. The different colors of data correspond to different laser intensities, as indicated in the legend in the upper right of the chart area.

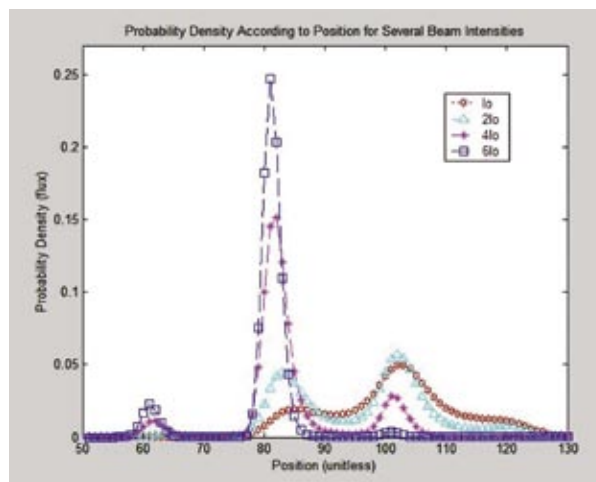


Figure 8: Probability density (flux) against position for increasing laser intensity. The different colors of data correspond to different laser intensities, as indicated in the legend in the upper right of the chart area.

three interference fringes) of the beam projected onto the sample was strictly uniform in nature. This limited the number of fringes having equal height through which the particle could fall to less than five. Interchanging the original lens with a second one with a longer focal length produced a larger area of uniform intensity, allowing a larger area to observe particle diffusion.

Control over all the parameters entering equation 4 would generate data covering a wide range of this parameter space. However, in these experiments there was no means to augment the force due to gravity. One other limitation (due to the brevity of this project) was the use of polystyrene particles 3 microns in diameter. The large size of these spheres suppressed the Brownian motion (i.e., last term in equation 4 is reduced).

Particle descent through the horizontal interference fringes was controlled by varying the output power of the argon laser while maintaining constant fringe spacing. Due to the exchange of lenses, particle descent was observed across a region of uniform beam intensity spanning roughly 10 interference fringes. Upon reaching the bottom, the sample was lifted back into uniform region; this procedure was repeated for several different values of power.

Results and Discussion

Samples were prepared using a highly diluted (more than one part per hundred) solution of three micron spherical polystyrene spheres in deionized water on immaculately clean glass slides. The sample was placed within a circularly cut region of double-sided Scotch tape to confine it to a small region of the slide

and also to adhere the two glass slides to one another. The sample was then placed on a mobile cantilever arm with three degrees of freedom. In order to acquire a group of particles for observation, the sample was left in the path of the laser operating at approximately 70 milliwatts for at least half an hour with either horizontal or vertical (but not both) fringe patterns intact. Particles eventually began to congregate near the intensity maxima at the center of the beam.

The data points in Figure 6 are of the average diffusion time of particles plotted against power. As can be seen, there is an exponential relationship between applied laser power and the diffusion time: with a linear increase in laser power, the average time that a particle takes to diffuse from one interference fringe to another increases at an exponential rate.

Diffusion of Spherical Polystyrene Particles through a Tilted Washboard Potential (*continued*)

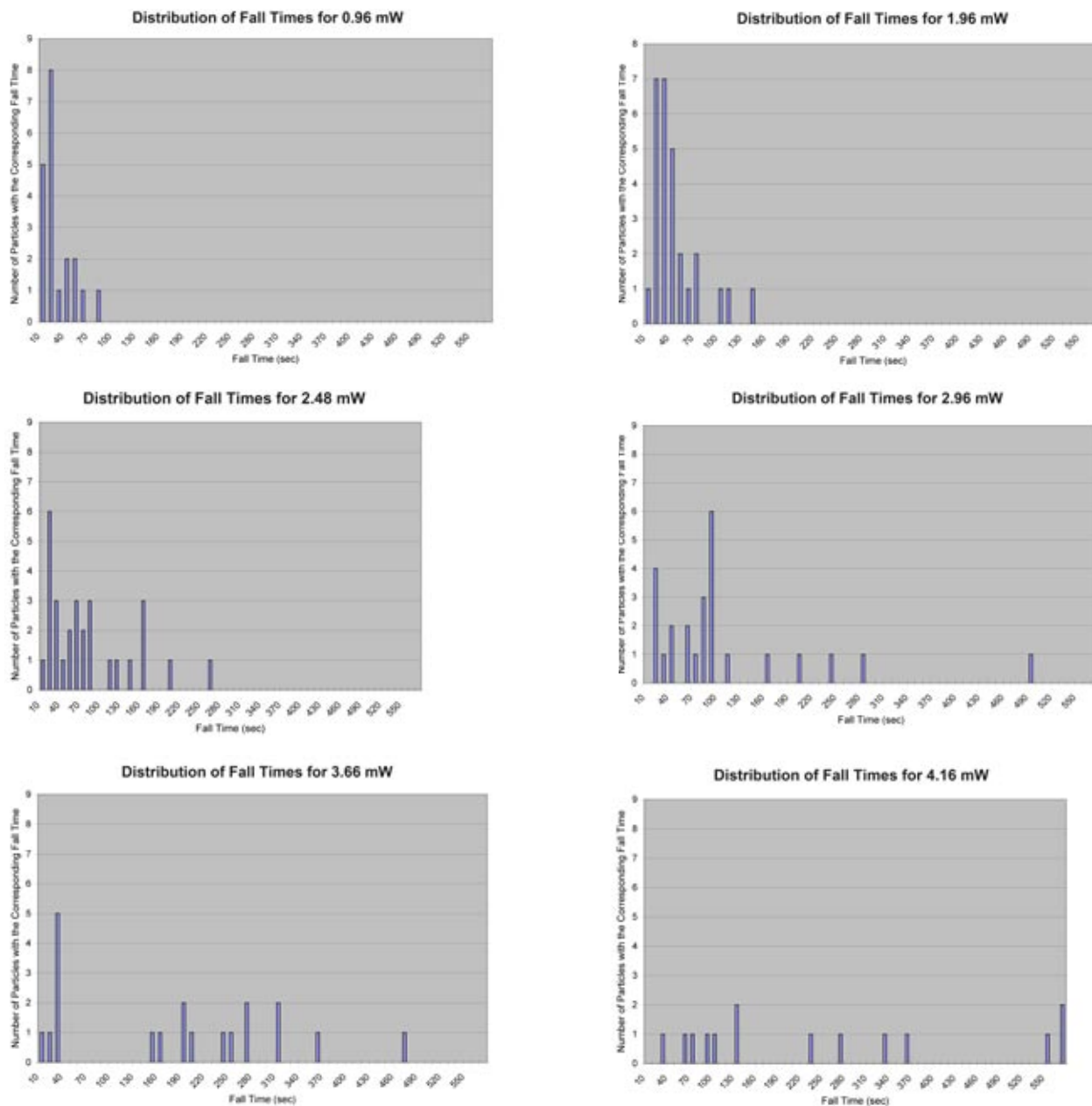


Figure 9: Distribution of particles taking corresponding times to diffuse with increasing laser intensity. Laser intensity increases from left to right, top to bottom.

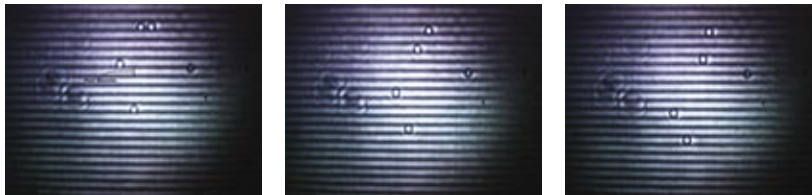


Figure 10: Three-shot progression of particle diffusion through interference fringes. The particle remaining towards the top of the interference pattern appears to be adhering to the glass slides. The rings to the left are particles not in the image plane of the interference pattern (out of focus).

The series of histograms shown in Figure 9 are of the number of particles taking a particular time to diffuse, plotted against time. At lowest intensity there is a localized distribution of particles diffusing in times under 10 seconds. As the laser power increased toward its maximum value, there was a far broader range of diffusion times, with some particles taking nearly 10 minutes to advance to the next interference fringe.

Tabulated data were compiled by numerically solving the one-dimensional diffusion equation 5 using the finite difference time domain (FDTD) method. Figure 6 shows the change-in-probability density with respect to time, plotted against time. Figure 7 shows the probability density plotted against position.

The simulated plot of Figure 8 against time reveals a bell curve, Gaussian in nature, which becomes broader with increasing laser power. As expected, this corresponds to particles spending more time confined within intensity maxima. The simulated plot against position reveals a curve with peaks that begin to contract and shift toward the origin. This corresponds to particles displacing less and less from their $t = 0$ position, and less broad distribution of displacements as the laser power is increased. The peaks correspond to the location of intensity maxima (multiples of five microns). As expected, this shows that the majority of

the particles spend the majority of time confined to intensity maxima, instead of intensity minima, or in transition between the two.

There is agreement between the trends shown in experimental and simulated data. There are, however, slight discrepancies between how the distributions change in the simulated data and how they change in the experimental data, which may be due to the use of approximations, including that observed particles are small in relation to the fringe spacing.

Conclusions

A great deal of data for the diffusion of three micron spherical polystyrene particles through five micron interference fringes was acquired, providing tools to characterize its motion. Additional data is needed to gain a smoother statistical plot of the particle probability density plotted against displacement, and the change in probability density with respect to time, plotted against time. However, preliminary data reveal that a linear increase in beam intensity yields an exponential increase in particle residence time of potential minima; this increase in power also yields a wider distribution of residence times and a contracted distribution of displacements (gradually converging to zero).

There was excellent agreement between the experimental data and the simulation results of the finite-difference time-

domain method. The only disagreement between the two sets of data stems from the fact that the default settings of the simulation run the environment with a point particle no larger than a few nanometers in diameter. Under these circumstances, Brownian motion is no longer negligible, as it is then comparable in magnitude to the force due to gravity and the gradient force of the laser. With three micron particles used in this study, Brownian motion did not show a consistent influence on the particle motion and accordingly was neglected.

References

- (1) Askin, A., et al. *Opt. Lett.* **1986**, *11*, 288.
- (2) Sasaki, K., et al. *Appl. Phys. Lett.* **1991**, *60*, 807.
- (3) Hirano, K., et al. *Appl. Phys. Lett.* **2002**, *80*, 515.
- (4) Ashkin, A. *Phys. Rev. Lett.* **1970**, *24*, 156.
- (5) Constantini, G.; Marchesoni, F. *Europhys. Lett.* **1999**, *48*, 491.
- (6) Kittel, C. *Elementary Statistical Physics*; Wiley: New York, **1958**; p 154.